Published in Applied Physics Letters, 105, issue 4, 043502/1-4, 2014
which should be used for any reference to this work

Microfabricated alkali vapor cell with anti-relaxation wall coating

R. Straessle,[1,a),b)] M. Pellaton,[2,a)] C. Affolderbach,[2] Y.P´etremand,[1,c)] D. Briand,[1] G. Mileti,[2,d)] and N. F. de Rooij[1,e)]
[1]*Institute of Microengineering (IMT), Sensors, Actuators and Microsystems Laboratory (SAMLAB), Ecole Polytechnique Fédérale de Lausanne (EPFL), 2000 Neuchâtel, Switzerland*
[2]*Laboratoire Temps-Fréquence (LTF), Institut de Physique, Université de Neuchâtel, 2000 Neuchâtel, Switzerland*

We present a microfabricated alkali vapor cell equipped with an anti-relaxation wall coating. The anti-relaxation coating used is octadecyltrichlorosilane and the cell was sealed by thin-film indium-bonding at a low temperature of 140 °C. The cell body is made of silicon and Pyrex and features a double-chamber design. Depolarizing properties due to liquid Rb droplets are avoided by confining the Rb droplets to one chamber only. Optical and microwave spectroscopy performed on this wall-coated cell are used to evaluate the cell's relaxation properties and a potential gas contamination. Double-resonance signals obtained from the cell show an intrinsic linewidth that is significantly lower than the linewidth that would be expected in case the cell had no wall coating but only contained a buffer-gas contamination on the level measured by optical spectroscopy. Combined with further experimental evidence this proves the presence of a working anti-relaxation wall coating in the cell. Such cells are of interest for applications in miniature atomic clocks, magnetometers, and other quantum sensors.

Microfabricated alkali vapor cells are widely studied and employed for miniature devices such as atomic magnetometers,[1] atomic clocks,[2,3] or other quantum sensors.[4] The required low relaxation rates of the atomic ground-state polarization are generally achieved by adding buffer gases to the cells, which results in decreased collision rates of the alkali atoms with the cell walls, longer ground-state polarization lifetime, and therefore improved stability in the case of an atomic clock. Alternatively, the lifetime of the polarization can be increased by depositing anti-relaxation coatings on the cell walls.[5–7] Macroscopic (∼few cm) alkali vapor cells equipped with anti-relaxation wall coatings have shown to be effective for the development of atomic clocks[5,8] and magnetometers.[9,10] Such coatings are also of interest for miniature atomic clocks[8,11,12] and several studies aimed at finding an optimal coating that is compatible with microfabrication,[11,13] in particular, in view of the elevated process temperatures.[14]

Three main groups of wall coatings with good anti-relaxation properties for alkali metals such as rubidium and cesium atoms are known: alkenes, alkanes, and organosilanes. Alkenes are the most efficient anti-relaxation coatings known so far, allowing more than 10^6 wall collisions of an alkali atom before depolarization.[15] However, their melting temperatures lie around 30 °C, well below typical working temperatures of mm-scale alkali vapor cells around 70 °C–100 °C. Alkane coatings show a shorter lifetime of the alkali spin polarization with up to 10^4 wall collisions before depolarization,[16,17] but with the advantage of higher melting temperatures (70 °C–90 °C). Organosilanes such as octadecyltrichlorosilane (OTS) show (due to the chemical bonds to the substrate sur-face and among each other) an increased temperature stability compared to alkene and alkane coatings, but allow up to 2000 wall collisions (for potassium atoms) at their best before depolarization.[13] OTS layers are stable up to 170 °C in the presence of Rb vapor, above which irreversible degradation occurs[11,13] and stable up to 230 °C in absence of alkali vapors.[18] They can be applied as self-assembled monolayer (SAM) or multilayers, with five times higher T1 relaxation times reported for multi-layers compared to monolayers.[7] OTS coatings have been combined with anodic bonding and post-activation of Cs pills to avoid the presence of the alkali vapor during bonding, but no conclusive proof of anti-relaxation properties of the final cell was reported.[19] It thus appears that the known anti-relaxation coatings are not compatible with the standard cell sealing technique of anodic bonding[12] that requires elevated temperatures (250 °C–400 °C) and high electric fields which also might degrade the quality of the coating.

In this work, we report on the fabrication of wall-coated micro-fabricated alkali vapor cells, using a recently published low-temperature indium thin-film bonding technique.[20] In the following, we describe the cell design, cell fabrication, and sealing technique for a cell with implemented OTS wall coating, followed by the spectroscopic characterization of the produced cell.

For the cell design a double-chamber approach was chosen, in which liquid alkali droplets are confined to a reservoir chamber, well separated from the probe chamber that features the wall coating. This avoids depolarization of the spin-polarized alkali atoms in the probe chamber that could occur if the atoms collided with (or got absorbed by) alkali droplets present on the chamber walls, similar to collisions with an uncoated part of the cell walls. In a buffer-gas cell, these depolarizing effects are minimized simultaneously by the alkali-gas collisions. In a wall-coated cell however, no buffer

[a)]R. Straessle and M. Pellaton contributed equally to this work.
[b)]R. Straessle is now with Sensirion AG, 8369 Stäfa, Switzerland.
[c)]Y. Pétremand is now with CSEM, Microsystems Technology Division, 2000 Neuchâtel, Switzerland.
[d)]Electronic mail: gaetano.mileti@unine.ch
[e)]Electronic mail: nico.derooij@epfl.ch

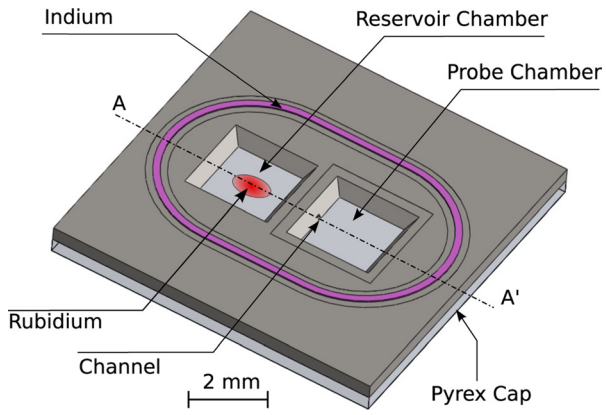

FIG. 1. Schematic view of the design of one cell preform with channel.

gas is present and thermal atoms undergo wall collisions at rates around 10^5–10^6 s^{-1} for mm-scale cells. Any fraction of the cell walls that is uncoated or covered by alkali droplets will thus lead to relaxation effects that scale with the area of the uncoated or alkali-covered surface.[21] To avoid this effect while ensuring a sufficient alkali vapor pressure in the probe chamber, in our cell the latter is linked to the reservoir chamber by a narrow channel of 100 × 100 μm^2 cross section.

Two cell preforms are bonded together by indium-bonding to obtain the cell. Both cell preforms are made of patterned silicon, anodically bonded to Pyrex (see Fig. 1). Each preform features two square chambers formed by KOH etching of Si, resulting in side lengths of 2 mm at the smaller openings. This allows for accurate dispensing of the alkali metal into the reservoir and for passing a narrow probe laser beam (0.56 mm diameter). One cell preform features the 100 × 100 μm^2 cross section channel that connects the reser-voir with the probe chamber. The metallization for the indium bonding is realized on both cell preforms and has an oval design to avoid metal accumulation in corners. The adhesion layer is 200 μm wide, consisting of 30 nm thick chromium and 50 nm gold. On one preform, the indium ring serving as seal is 200 μm wide and 4 μm high. On the second preform, there are three 12 μm wide indium rings with a height of 8 μm. When pressed together, the thin 12 μm rings cut into the 200 μm wide indium and a robust and hermetic bond is formed.[20] To avoid interaction of the alkali atoms with the indium at elevated temperatures, the area of possible interaction is minimized by placing the indium in 800 nm deep grooves.

When pressure is applied during bonding, the indium spreads out and the silicon surfaces of both sides get into close contact, leaving only a narrow opening for alkali vapor. A square area with a depth of 800 nm is etched around the probe chamber so that a thicker layer of coating would not prevent the silicon surfaces to be in contact after bonding.

Fabrication of the preforms for the alkali vapor cells was conducted on wafer level (see Fig. 2). Two different preform wafers were prepared, both consisting of a 390 μm silicon wafer bonded to a Pyrex wafer. The 800 nm grooves were etched with Deep Reactive Ion Etching (DRIE) on both wafers, while the 100 μm deep channels were etched by DRIE on the backside of only one wafer. The chambers were opened on both wafers with a wet etch in 40% KOH solution at 60 °C. The backside of the silicon wafers was bonded to 500 μm Pyrex wafers by anodic bonding. Then chromium and gold rings were formed by a lift-off process on the front side in the grooves. A second lift-off process was used to form the in-dium bond rings described above, with different dimensions on the two wafers. The wafers were protected with a layer of spray coated photoresist and diced into 10 × 10 mm^2 pre-forms. The protective layer was removed in acetone and the preforms rinsed in isopropanol before coating.

A thorough cleaning and outgassing step of the cell is required before coating with silanes to render the surface hydrophilic.[21] Due to the low melting point of indium, only a limited outgassing step could be performed. Furthermore, standard cleaning techniques like piranha solution (sulphuric acid:hydrogen peroxide in a 3:1 ratio) or RCA cleaning (three solutions: 13% (v/v) ammonium hydroxide, 2% (v/v) HF, 13% (v/v) hydrochloric acid) all etch indium and had therefore to be omitted. The applied compatible cleaning steps were cleaning in acetone and isopropanol alcohol and a 2 min oxygen plasma treatment, during which the indium was protected by a shadow mask to avoid excessive oxidation. The silicon wafer was then kept at ambient air for 4 h to allow the reaction of the -H endings of its natural silicon oxide layer to -OH.

It has been reported previously that OTS multilayer coatings show better anti-relaxation properties than OTS monolayers.[11] Therefore, our process of OTS coating was carried out in a laminar flow box at room temperature (22.3 °C) and ambient atmosphere; the water present in the atmosphere catalyzed the formation of OTS multilayers. A solution was prepared with 2 mM of OTS (from a freshly

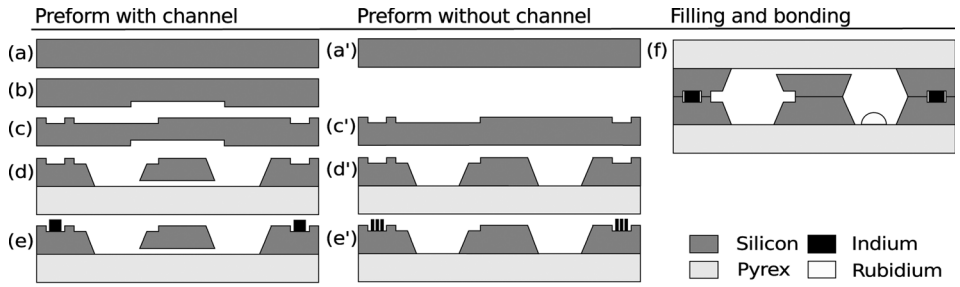

FIG. 2. Fabrication process—this view is a cut view along the line A-A′ of Fig. 1 through the channel. (a)/(a′) 390 μm thick Si wafer. (b) Etching of the channel by DRIE. (c)/(c′) Etching of grooves for metallization and coating by DRIE. (d)/(d′) KOH etching of chambers and anodic bonding of patterned silicon wafer to Pyrex. (e)/(e′) Metallization (adhesion layers and indium) by evaporation and lift-off process; dicing of the wafers; coating of the two cell preforms. (f) Rb is filled into the reservoir chamber of one cell preform, and the two preforms are bonded together by indium-bonding.

opened bottle) in toluene and stirred for 10 min. The preforms were immersed in the solution for 5 min. They were then rinsed thoroughly in pure toluene, blow-dried with a nitrogen gun, and kept in a dry atmosphere until used for cell fabrication. The OTS layers covered not only the plasma treated surface of the probe chamber but also partly the non-treated silicon and Pyrex and possibly also the indium. However, neither will the partly coated reservoir chamber have a negative effect on the performance nor will the potential nanometer coverage on the indium interfere with a successful bonding as the indium is squeezed out of its oxide shell during bonding.

The coverage of the OTS coating was deduced from two different measurements. A fully covered surface gives a water contact angle between 109° (Ref. 22) and 114° (Ref. 11). The water contact angle measured for our samples was 110°, corresponding to a coverage between 90% and 100%. The layer thickness measured by ellipsometry is an average over the measurement spot size and can therefore also be taken as a measure for the total coverage if the value for a complete layer is known. Assuming a refractive index of OTS of 1.465 and constant over wavelength, the resulting thickness of the OTS layer was 2.1 nm. Comparison to the lit-erature values for one complete monolayer[22] confirms cover-age of over 90%.

Cell sealing was performed by thermo-compression bonding in a dedicated machine for alkali cell fabrication.[23] A 2 h outgassing step at 100 °C was performed before bond-ing. A higher temperature would be preferred but the higher the temperature, the faster the interaction of the indium with the gold adhesion layer; the thin rings flow and broaden even below indium's melting temperature of 156 °C. After the outgassing, natural Rb was dispensed into the reservoir chamber and the cell was sealed by thin-film indium-bonding at 140 °C during 30 min with an applied tool pressure of 0.4 MPa.[20] A fully bonded cell with OTS coating and rubid-ium droplets is shown in Figure 3.

One produced cell was submitted to three spectroscopic tests[20] in order to evaluate its properties. In linear laser absorption spectroscopy, initially only the reservoir chamber showed Rb absorption lines. After several hours at 60 °C, also the probe chamber showed Rb absorption lines, confirming the presence of Rb vapor in the entire cell. From the absorption on resonance, the Rb number density in the reservoir chamber is

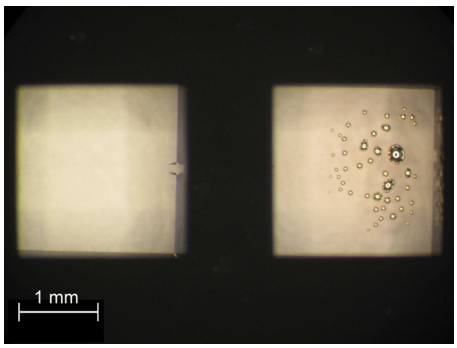

FIG. 3. Photograph of the double-chamber cell bonded by indium bonding with OTS coating. Rb droplets are visible only in the reservoir chamber (right-hand side).

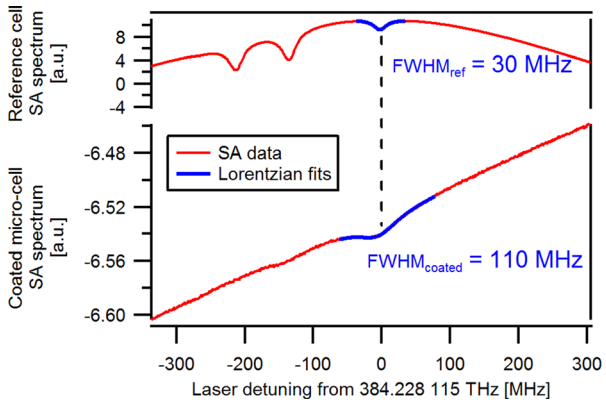

FIG. 4. SA optical spectra, recorded on an evacuated reference cell (upper trace) and in the probe chamber of the microfabricated cell (lower trace).

found to be twice as big as in the probe chamber, indicating a not fully achieved Rb density equilibration process or alkali absorption by the coating.[24] Saturated-absorption (SA) sub-Doppler spectroscopy[25] (see Figure 4) allows assessing a potential gas contamination in the cell via the collisional broadening of the optical transition.[26] The narrow SA feature observed on the coated microcell indicates an essentially collision-free regime and has a linewidth of 110 MHz, which is 80 MHz wider than for the reference cell spectrum. The additional broadening limits a potential gas contamination to few millibars, notably to $\leq$6 mbar for nitrogen assumed to be the most probable contaminating gas. Probing atoms near the coated surface in our thin cell might be an alternative origin of this broadening. For this nitrogen pressure level and our spe-cific cell geometry, a diffusion-limited Double-resonance (DR) linewidth of ~20 kHz would be expected.[21] Similar arguments apply for any buffer gas: for instance, an upper limit of 4 mbar can be given for H_2 that might originate from reactions between Rb and the silane coating,[27] resulting in even larger DR linewidths.[21,28]

DR signals of the Rb clock transition ($5^2S_{1/2}$, $F = 1, m_F = 0 \leftrightarrow F = 2, m_F = 0$) were recorded in the probe chamber using the setup described in Ref. 29, as shown in Figure 5. By extrapolation to zero light intensity, we find an intrinsic frequency shift of $\Delta\nu = -884 \pm 10$ Hz and an intrinsic linewidth of 8.9 ± 0.1 kHz. This linewidth is much less than the $\geq$20 kHz expected for the $\leq$6 mbar potential gas contamination, which is a strong indication for non-depolarizing wall

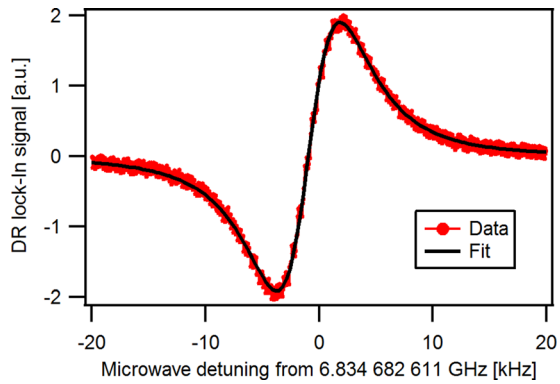

FIG. 5. Example of a typical DR signal observed in the cell's probe chamber. Due to the low signal contrast, lock-in detection was employed.

collisions due to the coating. A N_2 gas pressure of >24 mbar (and even higher for H_2) would be required to achieve a DR linewidth of <10 kHz in our cells, which is incompatible with the observed SA signals. Note that in our cell (4.2 mm^3 volume and 17.3 mm^2 wall area for one chamber), the rate of Rb collisions with the walls is $\gamma_{wall} \approx 2.95 \times 10^5\ s^{-1}$,[21] giving a DR linewidth around 95 kHz for an uncoated cell, which would make it almost impossible to observe a DR spectrum.

The observed 8.9 kHz intrinsic linewidth corresponds to an average Rb polarization lifetime of 35.8 μs, or the atomic polarization surviving $\approx$11 wall collisions. Assuming a perfect coating with only a small area uncoated, this corresponds to a $\approx$91% coverage of the surface,[21] which is consistent with the result from ellipsometric and contact angle measurements reported above. The reservoir effect due to the 100 μm $\times$ 100 μm cross-section channel in the microfabricated cell contributes a DR linewidth of less than 55 Hz.

The observed negative frequency shift $\Delta\nu$ of the clock transition is typical for coated cells,[21] and thus a second indication for the presence of a working wall coating. Most buffer gases induce a positive shift, e.g., $+404$ Hz/mbar for Nitrogen[30] assumed to be the most probable contaminating gas. Only few gases, like argon, krypton, or xenon, are known to induce negative shifts (-50 Hz/mbar, -437 Hz/mbar, and -890 Hz/mbar, respectively[30,31]), but as they are very rare gases that do not appear in the cell production process, they are excluded as contaminants here. Furthermore, a DR spectrum could only be obtained in the probe chamber, but not in the reservoir chamber. If any possible (even organic) buffer gas was responsible for the narrow linewidth observed, similar DR signals should be obtained in both chambers which are not observed. We therefore exclude that the narrow DR signal originates from a gas contamination in the cell, and attribute the absence of signal in the reservoir cell to the depolarizing properties of the Rb droplets present on the coated cell walls (see Fig. 3), and the reduced coating coverage. From the frequency shift $\Delta\nu$ of the clock transition, we calculate the average phase shift for an Rb atom-wall collision as $\phi = 2\pi\ \Delta\nu/\gamma_{wall} \approx -19$ mrad/collision, which is on the same order but significantly lower than the value of $\phi \approx -65$ mrad/collision extracted from OTS data given in Ref. 11.

In conclusion, we have presented a micro-fabricated Rb vapor cell sealed by low-temperature indium-bonding and equipped with OTS as anti-relaxation wall coating. The spectroscopic evaluation of the cell provides clear evidence that the observed narrow DR linewidths are caused by the presence of the coating, and they currently appear to be limited by the coating's coverage. These results thus prove the feasibility of wall-coated micro-fabricated alkali vapor cells, with application potential in atomic clocks, magnetometers, and other quantum instrumentation. Future studies could include a more detailed analysis of the coating, improvements in the coverage factor, and investigations on the long-term stability of the cells.

This work was supported by the Swiss National Science Foundation (Sinergia grant CRSI20-122693/1). M.P., C.A., and G.M. also acknowledge support from the European Space Agency (ESA) under the networking/partnering initiative (NPI) and the Swiss National Science Foundation Grant No. 200020_140681. The authors thank the CMI and the CSEM microsystems division staff and all the Sinergia project partners for their contributions and help.

[1] P. D. D. Schwindt, S. Knappe, V. Shah, L. Hollberg, J. Kitching, L.-A. Liew, and J. Moreland, Appl. Phys. Lett. **85**, 6409 (2004).
[2] S. Knappe, V. Shah, P. D. D. Schwindt, L. Hollberg, J. Kitching, L.-A. Liew, and J. Moreland, Appl. Phys. Lett. **85**, 1460 (2004).
[3] S. Knappe, Compr. Microsyst. **3**, 571 (2008).
[4] J. Kitching, S. Knappe, and E. A. Donley, IEEE J. Sens. **11**, 1749 (2011).
[5] H. G. Robinson and C. E. Johnson, Appl. Phys. Lett. **40**, 771 (1982).
[6] D. Budker, L. Hollberg, D. F. Kimball, J. Kitching, S. Pustelny, and V. V. Yashchuk, Phys. Rev. A **71**, 012903 (2005).
[7] S. J. Seltzer, D. M. Rampulla, S. Rivillon-Amy, Y. J. Chabal, S. L. Bernasek, and M. V. Romalis, J. Appl. Phys. **104**, 103116 (2008).
[8] T. Bandi, C. Affolderbach, and G. Mileti, J. Appl. Phys. **111**, 124906 (2012).
[9] G. Bison, R. Wynands, and A. Weis, Appl. Phys. B **76**, 325 (2003).
[10] D. Budker and M. Romalis, Nat. Phys. **3**, 227 (2007).
[11] Y. W. Yi, H. G. Robinson, S. Knappe, J. E. Maclennan, C. D. Jones, C. Zhu, N. A. Clark, and J. Kitching, J. Appl. Phys. **104**, 023534 (2008).
[12] J. Kitching, S. Knappe, and L. Hollberg, Appl. Phys. Lett. **81**, 553 (2002).
[13] S. J. Seltzer and M. V. Romalis, J. Appl. Phys. **106**, 114905 (2009).
[14] L.-A. Liew, S. Knappe, J. Moreland, H. Robinson, L. Hollberg, and J. Kitching, Appl. Phys. Lett. **84**, 2694 (2004).
[15] M. V. Balabas, T. Karaulanov, M. P. Ledbetter, and D. Budker, Phys. Rev. Lett. **105**, 070801 (2010).
[16] M. A. Bouchiat and J. Brossel, Phys. Rev. **147**, 41 (1966).
[17] S. Knappe and H. G. Robinson, New J. Phys. **12**, 065021 (2010).
[18] S. A. Mirji, Colloids Surf., A **289**, 133 (2006).
[19] A. Douahi, M. Hasegawa, L. Nieradko, J. J. Boy, C. Gorecki, and V. Giordano, in Proceedings of the 22nd European Frequency and Time Forum (EFTF), Toulouse, France, 22–25 April, 2008, FPE-0061.
[20] R. Straessle, M. Pellaton, C. Affolderbach, Y. P´etremand, D. Briand, G. Mileti, and N. F. de Rooij, J. Appl. Phys. **113**, 064501 (2013).
[21] J. Vanier and C. Audoin, *The Quantum Physics of Atomic Frequency Standards* (Adam Hilger, Bristol and Philadelphia, 1989).
[22] M.-H. Jung and H.-S. Choi, Korean J. Chem. Eng. **26**, 1778 (2009).
[23] Y. P´etremand, C. Affolderbach, R. Straessle, M. Pellaton, D. Briand, G. Mileti, and N. F. de Rooij, J. Micromech. Microeng. **22**, 025013 (2012). V.
[24] Liberman and R. J. Knize, Phys. Rev. A **34**, 5115 (1986).
[25] W. Demtr¨oder, *Laser Spectroscopy*, 4th ed. (Springer, Berlin Heidelberg, 2008), Vol. 2, pp. 94–104.
[26] M. D. Rotondaro and G. P. Perram, J. Quant. Spectrosc. Radiat. Transfer **57**, 497 (1997).
[27] J. Camparo, R. P. Frueholz, and B. Jaduszliwer, J. Appl. Phys. **62**, 676 (1987).
[28] R. J. McNeal, J. Chem. Phys. **37**, 2726 (1962).
[29] M. Pellaton, C. Affolderbach, Y. P´etremand, N. F. de Rooij, and G. Mileti, Phys. Scr. **T149**, 014013 (2012).
[30] J. Vanier, R. Kunski, N. Cyr, J. Y. Savard, and M. Tˆetu, J. Appl. Phys. **53**, 5387 (1982).
[31] B. H. McGuyer, T. Xia, Y.-Y. Jau, and W. Happer, Phys. Rev. A **84**, 030501(R) (2011).